

Bone Metastases in Patients with Metastatic Breast Cancer: Morphologic and Metabolic Monitoring of Response to Systemic Therapy with Integrated PET/CT¹

Ukihide Tateishi, MD
Cristina Gamez, MD
Shaheenah Dawood, MD
Henry W. D. Yeung, MD
Massimo Cristofanilli, MD
Homer A. Macapinlac, MD

Purpose: To retrospectively compare morphologic and metabolic changes in bone metastases in response to systemic therapy in patients with metastatic breast cancer (MBC) with integrated positron emission tomography (PET)/computed tomography (CT).

Materials and Methods: The institutional review board waived the requirement for informed consent and approved this HIPAA-compliant study. A retrospective analysis was performed with 102 women (mean age, 55 years) with MBC who received systemic treatment. All patients underwent integrated PET/CT before and after treatment. Two reviewers analyzed the images in consensus. Morphologic changes, including morphologic patterns, and lesion attenuation were evaluated. Standardized uptake value (SUV) and total lesion glycolysis (TLG) were analyzed to evaluate metabolic changes. Uni- and multivariate analyses were performed to identify factors that enabled response duration (RD) to be predicted.

Results: At baseline, the morphologic patterns of the target lesions were lytic ($n = 33$), sclerotic ($n = 22$), mixed ($n = 42$), and unclassified ($n = 5$). Progression of sclerotic change after treatment was identified in 49 patients (48%). After treatment, the mean attenuation of the lesion increased, whereas the mean SUV and TLG decreased. Increases in attenuation correlated significantly with decreases in SUV ($r = -0.510$, $P < .001$) and TLG ($r = -0.491$, $P < .001$). Univariate analysis revealed that the increase in attenuation and the decrease in SUV were potential predictors of RD. Multivariate analysis revealed that an increase in the change in SUV was a significant predictor of RD (relative risk, 2.4; $P = .003$).

Conclusion: A decrease in SUV after treatment was an independent predictor of RD in patients with MBC who had bone metastases.

© RSNA, 2008

¹ From the Department of Nuclear Medicine (U.T., C.G., H.W.D.Y., H.A.M.) and Division of Breast Medical Oncology (S.D., M.C.), University of Texas M.D. Anderson Cancer Center, Unit 1263, 1515 Holcombe Blvd, Houston, TX 77030. Received March 27, 2007; revision requested May 25; revision received May 31; accepted June 14; final version accepted September 17. Supported in part by grants from Scientific Research Expenses for Health and Welfare Programs and the Grant-in-Aid for Cancer Research from the Ministry of Health, Labor, and Welfare. Address correspondence to U.T. (e-mail: utateish@ncc.go.jp).

Bone is the most common site of distant metastasis, and metastases to bone are diagnosed in 30%–85% of patients with advanced breast cancer (1). Bone metastasis causes much of the morbidity and disability in patients with breast cancer because of its potentially prolonged clinical course. Proper assessment of treatment response is essential for making correct treatment decisions and improving outcome.

Fluorine 18 fluorodeoxyglucose (FDG) positron emission tomography (PET) has been shown to be substantially more accurate than conventional imaging in the assessment of functional tumor response to chemotherapy or hormone therapy in patients with primary breast cancer (2–5) and those with metastatic breast cancer (MBC) (6–9). Furthermore, the degree of the increase in glycolysis has been found to enable physicians to predict the outcome of breast cancer (10). Although PET has been proved to be an effective tool in the care of patients with breast cancer, it provides limited information on the morphologic abnormalities in bone. Three types of bone metastases (ie, lytic, sclerotic, and mixed) often complicate assessment of treatment outcome (10–13).

Accurately co-registered functional and morphologic data sets are generated with integrated PET/computed tomographic (CT) imaging systems, and the initial results for diagnosis of skeletal metastasis with this combined functional and morphologic system have been promising (14). However, despite the increasing use of integrated PET/CT in the management of breast cancer, to our knowledge, the clinical utility of combined assessment of FDG avidity

and morphologic changes in breast cancer metastases to bone has not been fully elucidated. Thus, the aim of our study was to retrospectively compare morphologic and metabolic changes in bone metastases in response to systemic therapy in patients with MBC with integrated PET/CT.

Materials and Methods

Patients

Our institutional review board waived the requirement for informed consent and approved our Health Insurance Portability and Accountability Act-compliant study. A retrospective search of our institutional PET/CT database revealed 162 women who were referred for staging of MBC and assessment of the response of MBC to treatment between June 2003 and August 2006. Sixty (37%) of the 162 patients originally identified as being eligible for this study were later excluded because they had a history of radiation therapy ($n = 20$), treatment with a granulocyte colony-stimulating factor or erythropoietin ($n = 17$), concomitant malignancy ($n = 17$), or diabetes ($n = 2$); because of a severe metal artifact ($n = 1$); or because PET/CT revealed no discernable lesions in patients in whom bone metastases had been identified with bone scintigraphy only or magnetic resonance (MR) imaging only ($n = 3$). Thus, a total of 102 patients (mean age, 55 years; age range, 25–89 years) with bone metastases from breast cancer were ultimately included.

Chemotherapy and hormone therapy were the preferred first-line treatments for MBC in this study. Hormone therapy consisted of administration of an estrogen receptor antagonist (tamoxifen) or an aromatase inhibitor. Chemotherapy alone was used to treat

widespread or life-threatening disease, and patients with negative estrogen receptor findings underwent only chemotherapy. Combined chemotherapy and hormone therapy was preformed in 76 patients, whereas 26 patients underwent only chemotherapy.

Imaging

PET/CT was performed prior to systemic therapy as a baseline study (mean, 11 days; range, 0–18 days) and after treatment (mean, 28 days; range, 21–38 days) in all patients. PET/CT images were acquired with an integrated PET/CT device (Discovery ST-8; GE Medical Systems, Milwaukee, Wis), and the whole-body mode was implemented as the standard software. Before PET/CT, the patients fasted for at least 6 hours. All patients were tested to confirm that their glucose level was within the normal range (80–120 mg/dL [4.4–6.6 mmol/L]) before FDG administration. Before PET, unenhanced CT was performed from the base of the skull to the upper thigh according to a standardized protocol performed with the following settings: transverse 3.75-mm section thickness, 140 kVp, 120 mA, and 13.5-mm table speed.

Emission scans were obtained 60 minutes after intravenous administration of FDG (mean dose, 555 MBq; range, 444–740 MBq). The acquisition time was

Advance in Knowledge

- A decrease in attenuation and an increase in standardized uptake value (SUV) of bone metastases after systemic therapy are associated with a markedly increased risk of disease progression in patients with metastatic breast cancer (MBC).

Implication for Patient Care

- A decrease in SUV of the lesion after systemic therapy was an independent predictor of response duration in patients with MBC who had bone metastasis.

Published online

10.1148/radiol.2471070567

Radiology 2008; 247:189–196

Abbreviations:

FDG = fluorine 18 fluorodeoxyglucose
MBC = metastatic breast cancer
RD = response duration
SUV = standardized uptake value
TLG = total lesion glycolysis

Author contributions:

Guarantors of integrity of entire study, all authors; study concepts/study design or data acquisition or data analysis/interpretation, all authors; manuscript drafting or manuscript revision for important intellectual content, all authors; manuscript final version approval, all authors; literature research, U.T., M.C., H.A.M.; clinical studies, all authors; statistical analysis, U.T.; and manuscript editing, U.T., H.W.D.Y., M.C., H.A.M.

Authors stated no financial relationship to disclose.

3 minutes per bed position in the two-dimensional mode. Images were reconstructed with attenuation-weighted ordered-subset expectation maximization with and without attenuation correction.

Image Interpretation and Morphologic Analyses

PET and CT images obtained in all standard planes were reviewed on an Advance workstation (GE Medical Systems). Two reviewers (U.T., C.G.; each with 2 years of experience) visually and quantitatively analyzed the images and recorded their findings after they reached a consensus. For visual analysis, abnormal FDG uptake was defined as substantially greater activity in tissue than in the aortic blood on attenuation-corrected images. Only the lesion that exhibited the most substantial uptake was selected as the target lesion for response to therapy. A region of interest (ROI) was outlined within areas of increased FDG uptake and measured on each section. When the lesion was extensively heterogeneous, the ROI was set to cover all lesion components.

When abnormal FDG uptake was present in bone, the exact anatomic location of the abnormal uptake was identified on CT images. Patients were classified as having lytic, sclerotic, mixed, or unclassified metastatic bone disease

at the time of diagnosis of bone metastasis on the basis of the findings of the CT portion of the PET/CT examination. Unclassified disease included the lesions that had minimal sclerotic or lytic change when compared with the adjacent bone. The morphologic changes observed on CT scans were classified as lytic-progressive change, sclerotic-progressive change, or structural change. The change in CT attenuation (ΔAtt) (measured in Hounsfield units) in the ROI of the entire lesion before and after treatment was calculated with the following equation: $\Delta\text{Att} = [(\text{Att}_{\text{pre}} - \text{Att}_{\text{post}}) / \text{Att}_{\text{pre}}] \cdot 100$, where Att_{pre} and Att_{post} denote pre- and posttreatment attenuation, respectively.

Standardized Uptake Value

The maximum standardized uptake value (SUV) was calculated with the following equation: $\text{SUV} = A / (\text{ID} / \text{BW})$, where A is the decay-corrected mean activity in tissue (measured in millicuries per milliliter), ID is the injected dose of FDG (measured in millicuries), and BW is the patient's body weight (measured in grams). Changes in SUV (ΔSUV) after treatment were calculated with the following equation: $\Delta\text{SUV} = [(\text{SUV}_{\text{pre}} - \text{SUV}_{\text{post}}) / \text{SUV}_{\text{pre}}] \cdot 100$, where SUV_{pre} and SUV_{post} denote pre- and posttreatment SUV, respectively.

Total Lesion Glycolysis

The change in total lesion glycolysis (ΔTLG), also called the Larson-Ginsberg index, was calculated as the response score (15) based on the volume (V) obtained with PET and the average SUV with use of the following equation: $\Delta\text{TLG} = \{[(\text{SUV}_{\text{pre}} \cdot V_{\text{pre}}) - (\text{SUV}_{\text{post}} \cdot V_{\text{post}})] / (\text{SUV}_{\text{pre}} \cdot V_{\text{pre}})\} \cdot 100$, where the subscripts "pre" and "post" refer to the pre- and posttreatment values, respectively.

Responders and Nonresponders

Two radiologists (U.T., C.G.) retrospectively reviewed the medical records for follow-up findings detected at visual analysis of PET/CT images, bone scintigrams, and MR images. In patients who were designated as responders, the target lesion showed decreased uptake when compared with the same lesion depicted on baseline images. In nonresponders, a follow-up examination revealed FDG uptake in the target lesion was substantially increased or similar to that seen previously. When the target lesion showed increased FDG uptake compared to the baseline value, bone scintigraphy and MR imaging were also performed. Increased FDG uptake in the target lesion, which was also substantially enlarged at MR imaging or had positive bone scintigraphy findings, was considered indicative of relapsed or progressive disease.

Table 1

Baseline Characteristics of Patients

Characteristic	Value
Mean age (y)*	55 ± 12 (25–89)
Primary tumor	
Unilateral	96 (94)
Bilateral	6 (6)
Treatment for bone metastasis	
Hormone therapy and chemotherapy	76 (75)
Chemotherapy alone	26 (25)
Distant metastasis in tissue other than bone	
Liver	32 (31)
Lung	23 (23)
Brain	17 (17)
Pleura	11 (11)
Other	8 (8)

Note.—Unless otherwise indicated, data are numbers of patients, and data in parentheses are percentages.

* Data are mean ± standard deviation. Data in parentheses are the range.

Table 2

Morphologic Findings at Baseline PET/CT

Parameter	No. of Patients
Distribution	
Medulla	62 (61)
Cortex and medulla	35 (34)
Unclear	5 (5)
Specific finding	
None	90 (88)
Formation of soft-tissue mass	7 (7)
Fracture	5 (5)
Periosteal reaction	1 (1)

Note.—Data in parentheses are percentages.

Figure 1

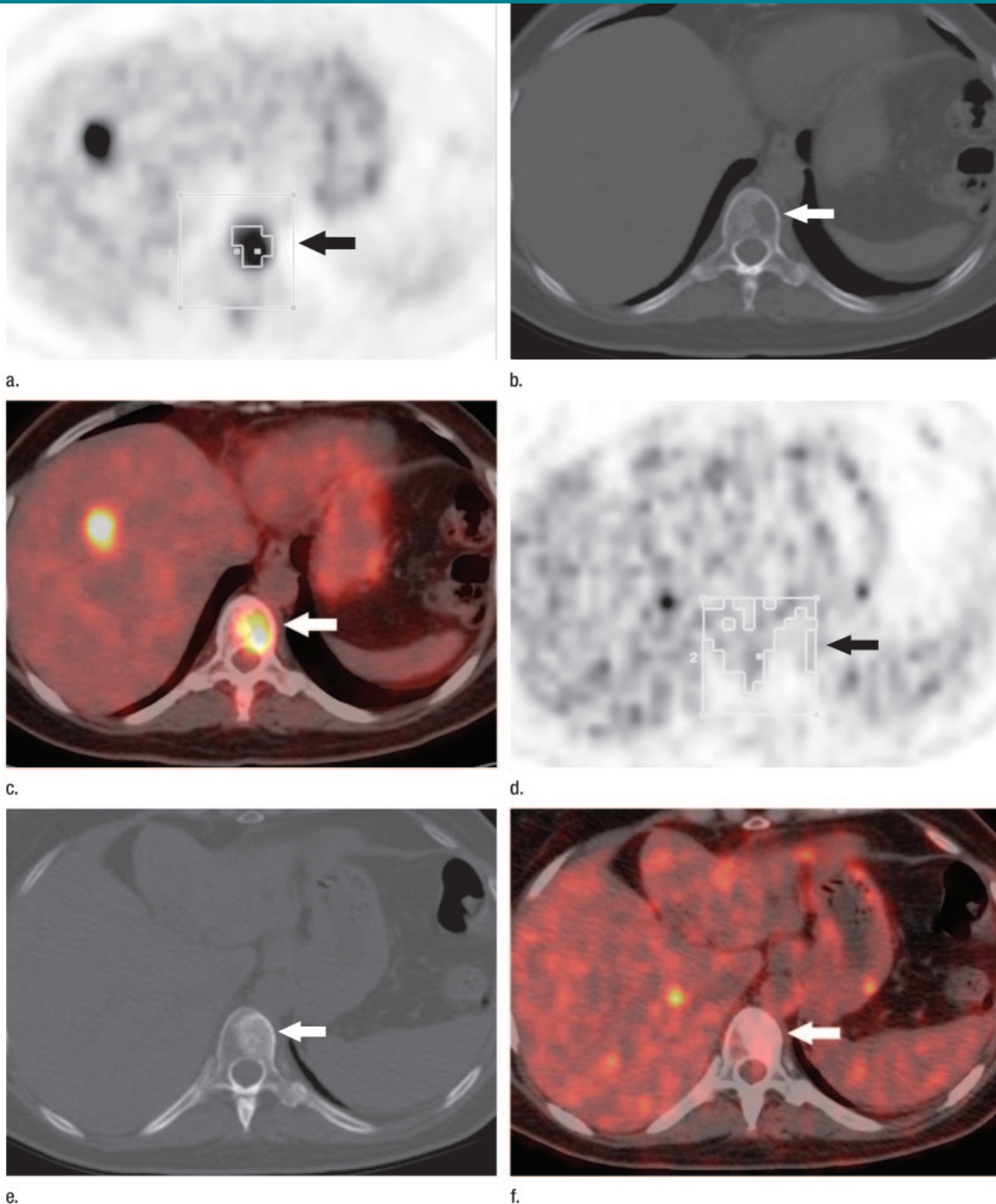


Figure 1: FDG PET, CT, and FDG PET/CT images obtained before and after systemic therapy. Baseline transaxial (a) FDG PET, (b) correlative CT, and (c) PET/CT images in a 49-year-old woman show bone metastasis in the thoracic spine at the level of the T11 vertebra (arrow). Mean values of attenuation, SUV, and TLG of the lesion are 268.4 HU, 7.9 g/mL, and 439.8, respectively. Abnormal FDG uptake in the liver corresponds to hepatic metastasis. Transaxial (d) FDG PET, (e) correlative CT, and (f) PET/CT images obtained 18 months after the start of hormone therapy and chemotherapy show progression of sclerotic change and metabolic reduction (arrow). Different abnormal FDG uptake in the liver corresponds to a new lesion of hepatic metastasis. Mean values of attenuation, SUV, and TLG of the lesion are 309.0 HU, 2.8 g/mL, and 338.1, respectively. Thus, the increase in attenuation was 15.1%, whereas the decreases in SUV and TLG were 64.6% and 23.1%, respectively.

Table 3

PET/CT Parameters at Baseline and After Treatment

Parameter	Baseline	After Treatment
Attenuation (HU)		
Mean*	284.6 ± 161.5	336.4 ± 197.8
Range	20.6–758.2	26.3–861.1
SUV (g/mL)		
Mean*	7.9 ± 5.6	7.2 ± 5.5
Range	2.0–26.7	1.5–26.2
TLG		
Mean*	50.9 ± 71.3	42.6 ± 38.9
Range	2.1–627.1	2.3–197.3

* Data are mean values ± standard deviations.

Table 4

Changes in PET/CT Parameters After Treatment

Parameter	Nonresponders (n = 50)	Responders (n = 52)	Overall	P Value
Change in attenuation (%)				
Mean*	-8.0 ± 56.8	-26.3 ± 52.4	-15.8 ± 54.5	.09
Range	-190.5 to 64.1	-229.2 to 23.6	-249.2 to 94.9	
Change in SUV (%)				
Mean*	-42.6 ± 81.8	12.5 ± 66.7	-16.1 ± 78.7	<.001
Range	-228.0 to 85.2	-239.0 to 77.4	-239.0 to 85.2	
Change in TLG (%)				
Mean*	-19.9 ± 73.8	-1.9 ± 61.5	-11.5 ± 68.2	.18
Range	-186.0 to 94.2	-197.9 to 90.4	-197.9 to 94.2	

Note.—Nonresponders were patients with a target lesion that showed substantial increase or a value similar to that seen previously. Responders were patients with a target lesion that showed decreased uptake compared with baseline values.

* With the exception of the P values, data are mean values ± standard deviations.

Statistical Analysis

Comparison of mean values between groups was performed with the Student *t* test. Response duration (RD), which was the period from the time at which the patients met the criteria to be considered responders to the time at which the event occurred as the first evidence of relapse or progression, was chosen as the end point for assessment of the prognostic value. The time of the initial diagnosis of bone metastasis was the starting time for the assessment of RD. Univariate regression analyses were performed to assess the cumulative hazard of disease progression by comparing Kaplan-Meier survival curves and performing log-rank tests. Multivariate Cox proportional hazards regression analyses were applied to test the independence of established prognostic factors in the prediction of disease progression. $P < .05$ was considered to indicate a significant difference. Statistical analysis was performed with SPSS software (version 12; SPSS, Chicago, Ill).

Results

Patients and Lesions

The median number of lesions per patient was four (range, 1–16 lesions per patient). At the time of initial diagnosis, target bone lesions were located in the spine ($n = 74$), ilium ($n = 15$), sternum ($n = 7$), pubis ($n = 2$), clavicle ($n = 1$),

humerus ($n = 1$), and femur ($n = 1$), as well as in a rib ($n = 1$). Fifty-seven patients (56%) had a distant metastasis in tissue other than bone at baseline (Table 1). Diagnoses consisted of invasive ductal carcinoma in 90 patients (88%) and lobar carcinoma in 12 (12%). Pathologic studies revealed that 82 patients (80%) had estrogen receptor-positive disease, 57 (56%) had progesterone receptor-positive disease, and 19 (19%) showed signs of *HER2* gene expression. After a median follow-up period of 15 months (range, 1–36 months), 77 patients (75%) were still alive, whereas 25 patients (25%) had died from their disease.

Target bone lesions (Table 2) were distributed in the medulla in 62 patients (61%) and in both the cortex and the medulla in 35 patients (34%). In five patients, the lesion seen on the CT portion of the PET/CT study was faint and its distribution was unclear. Specific findings were present in 13 patients (13%) and included formation of a soft-tissue mass ($n = 7$), fracture ($n = 5$), and periosteal reaction ($n = 1$). However, most patients ($n = 90$, 88%) did not have a specific finding.

Lesion Morphology and Follow-up

The morphologic pattern of the target lesions on the baseline PET/CT images was classified as lytic in 33 patients (32%), sclerotic in 22 (22%), mixed in 42 (41%), and unclassified in five (5%).

Figure 2

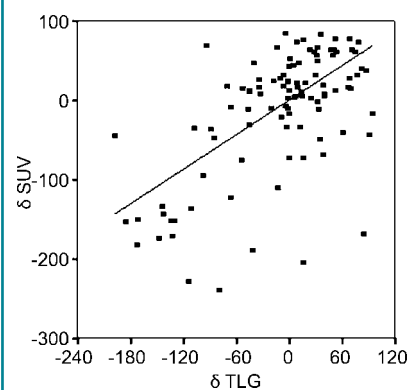


Figure 2: Scatterplot shows the relationship between SUV and TLG. The change in SUV was positively correlated with the change in TLG ($r = 0.614$, $P < .001$).

After treatment, however, the morphologic pattern of the target lesions was classified as lytic in 15 patients (15%), sclerotic in 35 (34%), mixed in 51 (50%), and unclassified in one patient (1%). Progression of sclerotic change after treatment (Fig 1) was identified in 49 patients (48%).

The mean attenuation of the lesion evaluated on the CT portion of the PET/CT study increased after treatment. In contrast, systemic therapy resulted in a decrease in the mean SUV and in the mean TLG when com-

pared with baseline values (Table 3). The decrease in SUV was significantly larger in responders than in nonresponders ($P < .001$, Table 4); however, no significant difference between responders and nonresponders was found for the increase in attenuation or the increase in TLG. There was a significant linear relationship between the decrease in SUV and the decrease in TLG ($r = 0.614$, $P < .001$; Fig 2). The increase in attenuation correlated significantly with the decrease in SUV ($r = -0.510$, $P < .001$; Fig 3) and the de-

crease in TLG ($r = -0.491$, $P < .001$; Fig 4).

Univariate analysis was performed by using variables that have been suggested to be associated with the incidence of progression (Table 5), and both the increase in attenuation and the decrease in SUV were identified as potential predictors of the incidence of progression (Fig 5). Patient age, primary tumor, treatment, distribution, specific findings, sclerotic change, and decrease in TLG did not add predictive value for incidence of progression. The final multivariate analysis revealed that a decrease in SUV of 8.5% or more was a significant predictor of RD (relative risk, 2.4; 95% confidence interval: 1.3, 4.4; $P = .003$).

Discussion

Our results showed that an increase in attenuation and a decrease in SUV of bone metastases after systemic treatment are associated with RD in patients with MBC. Uni- and multivariate Cox regression analyses showed that a decrease in SUV of 8.5% or more was a significant predictor of a long RD.

PET contributes to the detection of lytic bone metastasis, which is associated with a poorer prognosis than is sclerotic metastasis (10). The FDG avidity of bone metastases in patients with MBC depends on the metastasis type. We found that an increase in the attenuation of bone metastases correlates with a decrease in SUV or TLG. This finding appears to corroborate

Figure 3

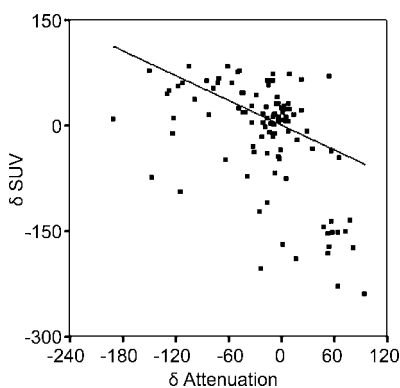


Figure 3: Scatterplot shows the relationship between attenuation and SUV. The increase in attenuation was negatively correlated with the decrease in SUV ($r = -0.510$, $P < .001$).

Figure 4

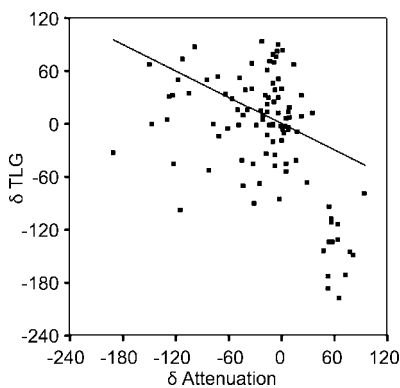


Figure 4: Scatterplot shows the relationship between attenuation and TLG. The increase in attenuation was negatively correlated with the decrease in TLG ($r = -0.491$, $P < .001$).

Table 5

Univariate Analysis of Progressive Disease after Systemic Therapy

Characteristic	No. of Patients	2-year Incidence of Progression (%)	P Value
Age (y)			.66
≥ 55	54	40	
< 55	48	48	
Primary tumor			.34
Unilateral	96	46	
Bilateral	6	33	
Treatment			.13
Hormone therapy and chemotherapy	76	41	
Chemotherapy alone	26	58	
Distribution			.82
Medulla	62	47	
Medulla and cortex	35	43	
Unclear	5	NA	
Specific findings			.86
Present	21	47	
Absent	81	44	
Sclerotic change			.14
Lesions exhibiting progression of sclerotic change	49	48	
Lesions with no progression of sclerotic change	53	34	
Change in attenuation (%)			$< .05$
Less than -8.6	49	33	
Greater than or equal to -8.6	53	44	
Change in SUV (%)			$< .01$
Less than 8.5	49	50	
Greater than or equal to 8.5	53	27	
Change in TLG (%)			.80
Less than -0.03	51	49	
Greater than or equal to -0.03	51	42	

Note.—NA = not applicable.

Figure 5

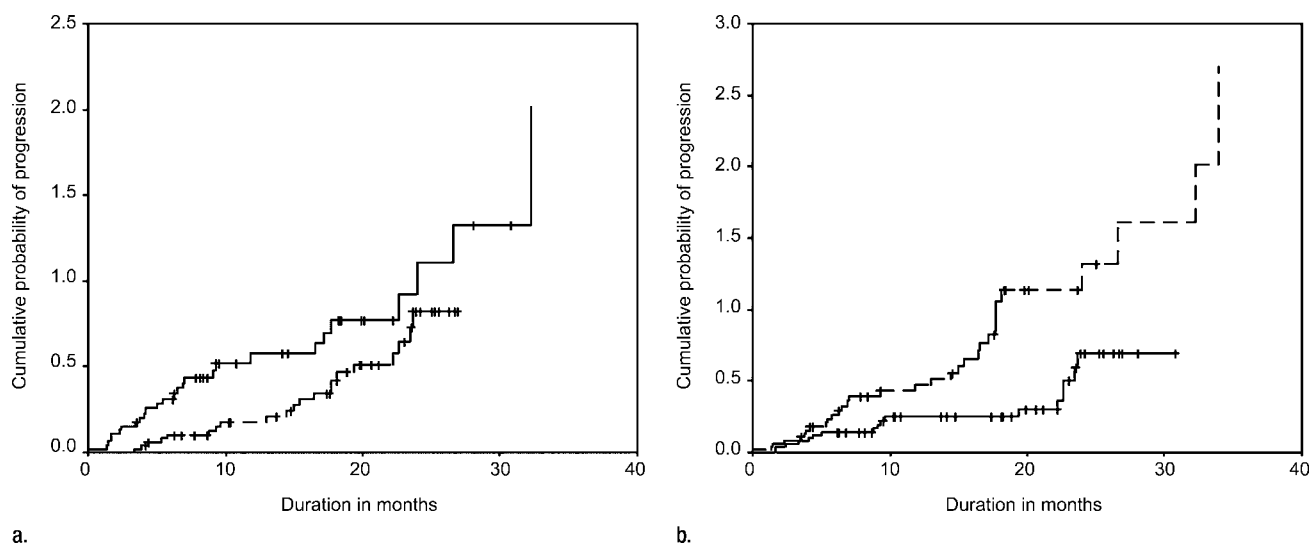


Figure 5: (a) Graph shows cumulative probability of progression of bone metastases in patients with an attenuation increase of 8.6% or more (solid line) and those with an attenuation increase of less than 8.6% (dashed line). A significant difference in cumulative hazard of progression was found between the groups at log-rank testing ($P < .05$). (b) Graph shows cumulative probability of progression of bone metastases in patients with an SUV decrease of 8.5% or more (solid line) and those with an SUV decrease of less than 8.5% (dashed line). A significant difference in cumulative hazard of progression was found between the groups at log-rank testing ($P < .01$).

the results of a previous study (15). Morphologic and metabolic assessment of bone metastasis with PET/CT can assist in monitoring the response to systemic therapy for bone metastases in patients with MBC.

Change in TLG (Δ TLG) is the ratio of the metabolic rate of the tumor at baseline to the metabolic rate of the tumor after treatment. Δ TLG corresponds to the change in the cell mass of the target lesion and reflects the global response of the entire tumor to treatment (15). In a study of 15 patients with rectal cancer, Δ TLG was shown to be a strong predictor of disease-specific and recurrence-free survival (16). It is important to note that other investigators found that Δ TLG reflected treatment response in patients with several types of locally advanced cancers and revealed information complementary to that obtained with SUV analysis. In contrast, our data showed that Δ TLG did not enable us to predict RD in patients who had bone metastases. The discrepancy between these findings may be related to the minimal changes in the volume of target bone lesions.

Metabolic reduction after treatment has been suggested to be of value in the

assessment of treatment efficacy in a variety of solid tumors (17–22). A change in tumor size after treatment is frequently used to evaluate therapeutic response in patients with breast cancer (23). However, patients with bone metastases have often been excluded from clinical trials because bone metastases are considered immeasurable. On the other hand, PET/CT enables semiquantitative assessment of uptake, which makes it convenient to use when evaluating tumor viability during treatment. Our findings showed that patients who had bone metastasis and metabolic reduction with an SUV decrease of 8.5% or more after treatment had a 2.4-fold higher relative risk of a long RD during follow-up.

In regard to the generation of data to aid in the prediction of outcome, the inclusion of patients who developed distant metastases to tissue other than bone during the course of the disease was a limitation of our study because the presence of distant metastases in other tissues can have a considerable effect on patient outcome. In a study of patients with advanced breast cancer, researchers found a wide variation in survival rates and showed that 20% of

the patients with bone metastases survived for more than 5 years (24). Therefore, we used RD as the primary end point to evaluate the value of PET/CT findings as a predictor of therapeutic efficacy.

Our study had other potential limitations. It may not have been sufficiently powered for the demonstration of significant differences among some of the covariates because we assessed only one target lesion per patient. However, the strength of our primary outcome, as well as the historic precedence of a significant predictor in the multivariate analysis, lends credence to our conclusions. Since data collection was performed retrospectively, selection bias may have affected our results. There may have been another aspect of bias in our study. The enrolled patients underwent one of two treatments for bone metastasis: (a) hormone therapy and chemotherapy and (b) chemotherapy alone. Further prospective studies are needed to assess the treatment effect of one standard regimen for bone metastasis with use of PET/CT. In our study, it was unclear whether PET/CT proved to be more cost-effective than conventional strategies. However, to our knowledge, the

costs and health outcomes associated with PET/CT in addition to those of conventional studies for MBC in clinical practice have not been assessed in the clinical or economic context. Clinical trials are needed to determine the cost-effectiveness of PET/CT in the care of patients with MBC.

In conclusion, our study results provide evidence that the change in SUV of bone metastasis after treatment is highly predictive of RD in patients with MBC. The predictive power of this parameter for long RD needs to be validated in a prospective study, and we plan to conduct such a study at our institution.

References

- Solomayer EF, Diel IJ, Meyberg GC, et al. Metastatic breast cancer: clinical course, prognosis, and therapy related to the first site of metastasis. *Breast Cancer Res Treat* 2000;59(3):271-278.
- Smith IC, Welch AE, Hutcheon AW, et al. Positron emission tomography using [(18)F]-fluorodeoxy-d-glucose to predict the pathologic response of breast cancer to primary chemotherapy. *J Clin Oncol* 2000;18(8):1676-1688.
- Schelling M, Avril N, Nahrig J, et al. Positron emission tomography using [(18)F]fluorodeoxyglucose for monitoring primary chemotherapy in breast cancer. *J Clin Oncol* 2000;18(8):1689-1695.
- Kim SJ, Kim SK, Lee ES, Ro J, Kang S. Predictive value of [18F]FDG PET for pathological response of breast cancer to neoadjuvant chemotherapy. *Ann Oncol* 2004;15(9):1352-1357.
- Rousseau C, Devillers A, Sagan C, et al. Monitoring of early response to neoadjuvant chemotherapy in stage II and III breast cancer by [18F]fluorodeoxyglucose positron emission tomography. *J Clin Oncol* 2006;24(34):5366-5372.
- Jansson T, Westlin JE, Ahlstrom H, Lilja A, Langstrom B, Bergh J. Positron emission tomography studies in patients with locally advanced and/or metastatic breast cancer: a method for early therapy evaluation? *J Clin Oncol* 1995;13(6):1470-1477.
- Gennari A, Donati S, Salvadori B, et al. Role of 2-[18F]-fluorodeoxyglucose (FDG) positron emission tomography (PET) in the early assessment of response to chemotherapy in metastatic breast cancer patients. *Clin Breast Cancer* 2000;1(2):156-161.
- Dose Schwarz J, Bader M, Jenicke L, Hemminger G, Janicke F, Avril N. Early prediction of response to chemotherapy in metastatic breast cancer using sequential 18F-FDG PET. *J Nucl Med* 2005;46(7):1144-1150.
- Couturier O, Jerusalem G, N'Guyen JM, Hustinx R. Sequential positron emission tomography using [18F]fluorodeoxyglucose for monitoring response to chemotherapy in metastatic breast cancer. *Clin Cancer Res* 2006;12(21):6437-6443.
- Cook GJ, Houston S, Rubens R, et al. Detection of bone metastases in breast cancer by 18FDG PET: differing metabolic activity in osteoblastic and osteolytic lesions. *J Clin Oncol* 1998;16(10):3375-3379.
- Nakamoto Y, Cohade C, Tatsumi M, Hammoud D, Wahl RL. CT appearance of bone metastases detected with FDG PET as part of the same PET/CT examination. *Radiology* 2005;237(2):627-634.
- James JJ, Evans AJ, Pinder SE, et al. Bone metastases from breast carcinoma: histopathological-radiological correlations and prognostic features. *Br J Cancer* 2003;89(4):660-665.
- Hamaoka T, Madewell JE, Podoloff DA, Hortobagyi GN, Ueno NT. Bone imaging in metastatic breast cancer. *J Clin Oncol* 2004;22(14):2942-2953.
- Beyer T, Townsend DW, Brun T, et al. A combined PET/CT scanner for clinical oncology. *J Nucl Med* 2000;41(8):1369-1379.
- Larson SM, Erdi Y, Akhurst T, et al. Tumor treatment response based on visual and quantitative changes in global tumor glycolysis using PET-FDG imaging: the visual response score and the change in total lesion glycolysis. *Clin Positron Imaging* 1999;2(3):159-171.
- Guillem JG, Moore HG, Akhurst T, et al. Sequential preoperative fluorodeoxyglucose-positron emission tomography assessment of response to preoperative chemoradiation: a means for determining longterm outcomes of rectal cancer. *J Am Coll Surg* 2004;199(1):1-7.
- Lowe VJ, Dunphy FR, Varvares M, et al. Evaluation of chemotherapy response in patients with advanced head and neck cancer using [F-18]fluorodeoxyglucose positron emission tomography. *Head Neck* 1997;19(8):666-674.
- Downey RJ, Akhurst T, Ilson D, et al. Whole body 18FDG-PET and the response of esophageal cancer to induction therapy: results of a prospective trial. *J Clin Oncol* 2003;21(3):428-432.
- Ott K, Fink U, Becker K, et al. Prediction of response to preoperative chemotherapy in gastric carcinoma by metabolic imaging: results of a prospective trial. *J Clin Oncol* 2003;21(24):4604-4610.
- Stroobants S, Goeminne J, Seegers M, et al. 18FDG-positron emission tomography for the early prediction of response in advanced soft tissue sarcoma treated with imatinib mesylate (Glivec). *Eur J Cancer* 2003;39(14):2012-2020.
- Pottgen C, Levegrun S, Theegarten D, et al. Value of 18F-fluoro-2-deoxy-d-glucose-positron emission tomography/computed tomography in non-small-cell lung cancer for prediction of pathologic response and times to relapse after neoadjuvant chemoradiotherapy. *Clin Cancer Res* 2006;12(1):97-106.
- Kalff V, Duong C, Drummond EG, Matthews JP, Hicks RJ. Findings on 18F-FDG PET scans after neoadjuvant chemoradiation provides prognostic stratification in patients with locally advanced rectal carcinoma subsequently treated by radical surgery. *J Nucl Med* 2006;47(1):14-22.
- Wahl RL, Zasadny K, Helvie M, Hutchins GD, Weber B, Cody R. Metabolic monitoring of breast cancer chemohormonotherapy using positron emission tomography: initial evaluation. *J Clin Oncol* 1993;11(11):2101-2111.
- Coleman RE, Rubens RD. The clinical course of bone metastases from breast cancer. *Br J Cancer* 1987;55(1):61-66.

Radiology 2008

This is your reprint order form or pro forma invoice

(Please keep a copy of this document for your records.)

Reprint order forms and purchase orders or prepayments must be received 72 hours after receipt of form either by mail or by fax at 410-820-9765. It is the policy of Cadmus Reprints to issue one invoice per order.

Please print clearly.

Author Name _____
Title of Article _____
Issue of Journal _____ Reprint # _____ Publication Date _____
Number of Pages _____ KB # _____ Symbol Radiology
Color in Article? Yes / No (Please Circle)

Please include the journal name and reprint number or manuscript number on your purchase order or other correspondence.

Order and Shipping Information

Reprint Costs (Please see page 2 of 2 for reprint costs/fees.)

_____ Number of reprints ordered \$ _____
_____ Number of color reprints ordered \$ _____
_____ Number of covers ordered \$ _____
Subtotal \$ _____
Taxes \$ _____

(Add appropriate sales tax for Virginia, Maryland, Pennsylvania, and the District of Columbia or Canadian GST to the reprints if your order is to be shipped to these locations.)

First address included, add \$32 for
each additional shipping address \$ _____

TOTAL \$ _____

Shipping Address (cannot ship to a P.O. Box) Please Print Clearly

Name _____
Institution _____
Street _____
City _____ State _____ Zip _____
Country _____
Quantity _____ Fax _____
Phone: Day _____ Evening _____
E-mail Address _____

Additional Shipping Address* (cannot ship to a P.O. Box)

Name _____
Institution _____
Street _____
City _____ State _____ Zip _____
Country _____
Quantity _____ Fax _____
Phone: Day _____ Evening _____
E-mail Address _____

* Add \$32 for each additional shipping address

Payment and Credit Card Details

Enclosed: Personal Check _____
Credit Card Payment Details _____
Checks must be paid in U.S. dollars and drawn on a U.S. Bank.
Credit Card: VISA Am. Exp. MasterCard
Card Number _____
Expiration Date _____
Signature: _____

Please send your order form and prepayment made payable to:

Cadmus Reprints
P.O. Box 751903
Charlotte, NC 28275-1903

Note: Do not send express packages to this location, PO Box.
FEIN #:541274108

Signature _____ Date _____

Signature is required. By signing this form, the author agrees to accept the responsibility for the payment of reprints and/or all charges described in this document.

Invoice or Credit Card Information

Invoice Address Please Print Clearly

Please complete Invoice address as it appears on credit card statement

Name _____
Institution _____
Department _____
Street _____
City _____ State _____ Zip _____
Country _____
Phone _____ Fax _____
E-mail Address _____

**Cadmus will process credit cards and Cadmus Journal
Services will appear on the credit card statement.**

*If you don't mail your order form, you may fax it to 410-820-9765 with
your credit card information.*

Radiology 2008

Black and White Reprint Prices

Domestic (USA only)						
# of Pages	50	100	200	300	400	500
1-4	\$221	\$233	\$268	\$285	\$303	\$323
5-8	\$355	\$382	\$432	\$466	\$510	\$544
9-12	\$466	\$513	\$595	\$652	\$714	\$775
13-16	\$576	\$640	\$749	\$830	\$912	\$995
17-20	\$694	\$775	\$906	\$1,017	\$1,117	\$1,220
21-24	\$809	\$906	\$1,071	\$1,200	\$1,321	\$1,471
25-28	\$928	\$1,041	\$1,242	\$1,390	\$1,544	\$1,688
29-32	\$1,042	\$1,178	\$1,403	\$1,568	\$1,751	\$1,924
Covers	\$97	\$118	\$215	\$323	\$442	\$555

Color Reprint Prices

Domestic (USA only)						
# of Pages	50	100	200	300	400	500
1-4	\$223	\$239	\$352	\$473	\$597	\$719
5-8	\$349	\$401	\$601	\$849	\$1,099	\$1,349
9-12	\$486	\$517	\$852	\$1,232	\$1,609	\$1,992
13-16	\$615	\$651	\$1,105	\$1,609	\$2,117	\$2,624
17-20	\$759	\$787	\$1,357	\$1,997	\$2,626	\$3,260
21-24	\$897	\$924	\$1,611	\$2,376	\$3,135	\$3,905
25-28	\$1,033	\$1,071	\$1,873	\$2,757	\$3,650	\$4,536
29-32	\$1,175	\$1,208	\$2,122	\$3,138	\$4,162	\$5,180
Covers	\$97	\$118	\$215	\$323	\$442	\$555

International (includes Canada and Mexico)						
# of Pages	50	100	200	300	400	500
1-4	\$272	\$283	\$340	\$397	\$446	\$506
5-8	\$428	\$455	\$576	\$675	\$784	\$884
9-12	\$580	\$626	\$805	\$964	\$1,115	\$1,278
13-16	\$724	\$786	\$1,023	\$1,232	\$1,445	\$1,652
17-20	\$878	\$958	\$1,246	\$1,520	\$1,774	\$2,030
21-24	\$1,022	\$1,119	\$1,474	\$1,795	\$2,108	\$2,426
25-28	\$1,176	\$1,291	\$1,700	\$2,070	\$2,450	\$2,813
29-32	\$1,316	\$1,452	\$1,936	\$2,355	\$2,784	\$3,209
Covers	\$156	\$176	\$335	\$525	\$716	\$905

International (includes Canada and Mexico))						
# of Pages	50	100	200	300	400	500
1-4	\$278	\$290	\$424	\$586	\$741	\$904
5-8	\$429	\$472	\$746	\$1,058	\$1,374	\$1,690
9-12	\$604	\$629	\$1,061	\$1,545	\$2,011	\$2,494
13-16	\$766	\$797	\$1,378	\$2,013	\$2,647	\$3,280
17-20	\$945	\$972	\$1,698	\$2,499	\$3,282	\$4,069
21-24	\$1,110	\$1,139	\$2,015	\$2,970	\$3,921	\$4,873
25-28	\$1,290	\$1,321	\$2,333	\$3,437	\$4,556	\$5,661
29-32	\$1,455	\$1,482	\$2,652	\$3,924	\$5,193	\$6,462
Covers	\$156	\$176	\$335	\$525	\$716	\$905

Minimum order is 50 copies. For orders larger than 500 copies, please consult Cadmus Reprints at 800-407-9190.

Reprint Cover

Cover prices are listed above. The cover will include the publication title, article title, and author name in black.

Shipping

Shipping costs are included in the reprint prices. Domestic orders are shipped via UPS Ground service. Foreign orders are shipped via a proof of delivery air service.

Multiple Shipments

Orders can be shipped to more than one location. Please be aware that it will cost \$32 for each additional location.

Delivery

Your order will be shipped within 2 weeks of the journal print date. Allow extra time for delivery.

Tax Due

Residents of Virginia, Maryland, Pennsylvania, and the District of Columbia are required to add the appropriate sales tax to each reprint order. For orders shipped to Canada, please add 7% Canadian GST unless exemption is claimed.

Ordering

Reprint order forms and purchase order or prepayment is required to process your order. Please reference journal name and reprint number or manuscript number on any correspondence. You may use the reverse side of this form as a proforma invoice. Please return your order form and prepayment to:

Cadmus Reprints
P.O. Box 751903
Charlotte, NC 28275-1903

Note: Do not send express packages to this location, PO Box. FEIN #: 541274108

Please direct all inquiries to:

Rose A. Baynard
800-407-9190 (toll free number)
410-819-3966 (direct number)
410-820-9765 (FAX number)
baynardr@cadmus.com (e-mail)

Reprint Order Forms and purchase order or prepayments must be received 72 hours after receipt of form.